Effect of Asphaltene Structure on Association and Aggregation Using Molecular Dynamics

ARTICLE *in* THE JOURNAL OF PHYSICAL CHEMISTRY B · APRIL 2013

Impact Factor: 3.3 · DOI: 10.1021/jp401584u · Source: PubMed

4 AUTHORS, INCLUDING:

Mohammad Sedghi
University of Wyoming
9 PUBLICATIONS **116** CITATIONS

SEE PROFILE

Lamia Goual
University of Wyoming
32 PUBLICATIONS **552** CITATIONS

SEE PROFILE

William R.W. Welch
University of Wyoming
14 PUBLICATIONS **94** CITATIONS

SEE PROFILE

THE JOURNAL OF PHYSICAL CHEMISTRY B

Article

pubs.acs.org/JPCB

Effect of Asphaltene Structure on Association and Aggregation Using Molecular Dynamics

Mohammad Sedghi,[†] Lamia Goual,*[,†] William Welch,[‡] and Jan Kubelka[‡]

[†]Department of Chemical and Petroleum Engineering and [‡]Department of Chemistry, University of Wyoming, 1000 East University Avenue, Laramie, Wyoming 82071, United States

ABSTRACT: The aggregation of asphaltenes has been established for decades by numerous experimental techniques; however, very few studies have been performed on the association free energy and asphaltene aggregation in solvents. The lack of reliable and coherent data on the free energy of association and aggregation size of asphaltene has imposed severe limitations on the thermodynamic modeling of asphaltene phase behavior. Current thermodynamic models either consider asphaltenes as non-associating components or use fitting parameters to characterize the association. In this work, the relations between Gibbs free energy of asphaltene association and asphaltene molecular structure are studied using molecular dynamics (MD). The free energy of association is computed from the potential of mean force profile along the separation distance between the centers of mass of two asphaltene molecules using the umbrella sampling technique in the GROMACS simulation package. The average aggregation number for asphaltene nanoaggregates and clusters is also calculated through MD simulations of 36 asphaltene molecules in toluene and heptane in order to estimate the effects of association free energy and steric repulsion on the aggregation behavior of asphaltenes. Our simulation results confirm that the interactions between aromatic cores of asphaltene molecules are the major driving force for association as the energy of association increases substantially with the number of aromatic rings. Moreover, heteroatoms attached to the aromatic cores have much more influence on the association free energy than to ones attached to the aliphatic chains. The length and number of aliphatic chains do not seem to have a noticeable effect on asphaltene dimerization; however, they have a profound effect on asphaltene aggregation size since steric repulsion can prevent asphaltenes from forming T-shape configurations and therefore decrease the aggregation size of asphaltenes significantly. Our MD simulation results show for the first time asphaltene precipitation in heptane as an explicit solvent, and predict three distinct stages of aggregation (nanoaggregation, clustering, and flocculation) as proposed by the modified Yen model. Finally, the association free energy for asphaltenes in heptane is higher than that in toluene, which is consistent with asphaltene aggregate sizes obtained from MD simulations.

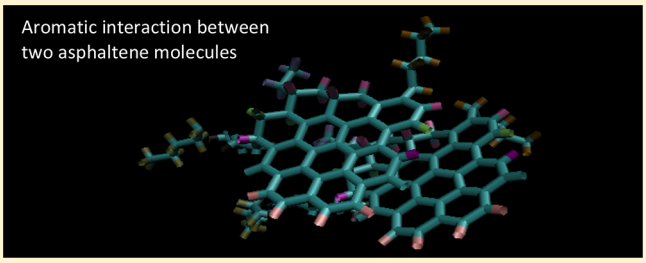

1. INTRODUCTION

Petroleum fluid is a mixture of a broad spectrum of constituents, having small molecules on one end and much larger and more polar aromatic molecules on the other end. Asphaltenes, which fall on the heavier end of the spectrum, are a solubility class typically defined as heptane-insoluble, toluene-soluble fraction of petroleum. Asphaltene molecules have an average molecular weight of 750 g/mol: one aromatic core consisting of 4−10 aromatic rings and peripheral aliphatic chains with lengths ranging from 3 to 7 carbons.[1−3] Asphaltene molecules have a high tendency to associate into larger aggregates. Their stability in petroleum fluids can be disrupted by pressure drop or compositional changes, which lead to asphaltene precipitation and deposition in subsurface formations, wellbores, or transportation pipelines.[4,5]

Successful thermodynamic prediction of asphaltene precipitation requires the understanding of asphaltene aggregation in terms of mechanism and aggregation strength. Without this fundamental knowledge, any attempt to model asphaltene phase behavior would be incomplete and/or inaccurate. For instance, PC-SAFT equation of state (EOS) has been used by Chapman research group[6−8] to predict asphaltene precipitation under carbon dioxide and miscible gas injection. Asphaltenes were considered as nanoaggregates so that dispersion forces would control their phase behavior. The size of these nanoaggregates was a fitting parameter to match titration data. Furthermore, the energy of asphaltene association was considered the same as the energy of covalent bonding. In cubic plus association EOS, Li and Firoozabadi[9,10] recently combined Peng−Robinson EOS with the Wertheim association formulation to model asphaltene phase behavior with molecular parameters. The parameters describing association interaction between asphaltenes had to be assumed since there were no data available in the literature.

The accurate modeling of asphaltene macroscale thermodynamic behavior necessitates the understanding of its microscale aggregation mechanism. Thus, a clear picture of the intermolecular forces involved in aggregation is a prerequisite.

Received: February 13, 2013
Revised: March 28, 2013
Published: April 12, 2013

Recently, a modified Yen model (also called Yen−Mullins model) has emerged based on the Yen model proposed in 1967.[1,2] This model stipulates that asphaltene nanoaggregates consist of less than 10 molecules stacked on top of each other. The aggregation stops beyond nanoaggregation; however, nanoaggregates can coagulate due to their high molar weight forming clusters of aggregates, which can eventually lead to flocculation. The driving force of aggregation is the $\pi-\pi$ stacking or aromatic interactions from the aromatic core of asphaltenes, and the force limiting their aggregation is the steric hindrance caused by aliphatic side chains. Aromatic interactions occur due to electrostatic attraction between the negative π electron cloud and positive σ frame of aromatic rings.[11,12] Three configurations for aromatic interactions have been confirmed: face-to-face or parallel, offset stacking or offset parallel, and edge-to-face or T-shape. The most stable conformation for benzene dimers is edge-to-face in order to minimize the repulsion between the electron clouds; however, as the number of fused rings increases in a molecule, the parallel or offset parallel formation becomes more favorable. Rodriguez et al.[13] used molecular mechanics (MM) to study the aromatic interactions between coronene molecules in a vacuum and found that coronene dimers would have a lower energy forming offset stacking than T-shape configuration.

Several studies have focused on the determination of interaction energies between asphaltene-like molecules. Among the earlier works in a vacuum, Rogel[14] used an energy minimization method with the Consistent Valence Force Field[15] to calculate asphaltene dimer interaction and stabilization energies from four different crude oils. For each asphaltene molecule, the stabilization and interaction energies were found to be close and in the range of −100 to −200 kcal/mol in a vacuum. This study also suggested that hydrogen-bonding, heteroatom functional groups, and intermolecular conformational changes play no significant role in the stabilization of asphaltene dimers and the main force of association is the van der Waals interaction ($\pi-\pi$ interactions). Another conclusion was that asphaltene molecules with higher aromaticity, lower H/C ratio, and higher molecular weight have more stable dimers. In a more recent study using COMPASS Force Field (FF),[16−19] Pacheco-Sánchez et al.[20] obtained the dimerization energy of a model asphaltene molecule in a vacuum and found that dimers have a potential well depth of about −55 kcal/mol when their center of mass (COM) distance is between 3 and 4 Å and their aromatic cores are parallel to each other. Using MM and semiempirical quantum calculations, Carauta et al.[3] obtained the interaction energy between enantiomers of two asphaltene structural models having a hydroxyl functional group and found the stabilization energy of asphaltene dimers to be smaller than 45 kcal/mol in a vacuum. Also, the authors did not observe any H-bonding between asphaltenes. Alvarez-Ramirez et al.[21] combined classical MM and quantum mechanics (QM) to calculate the binding energy between asphaltene-like molecules. They used two Density Functional Theory (DFT) methods (namely Harrison Functional and PW91)[22,23] in QM and the COMPASS FF in classical MM. On the basis of their results, they estimated the binding energy between asphaltene molecules in a vacuum to be about −12 to −15 kcal/mol.

Little work has been performed on the dimerization free energy of asphaltenes in solvents. Ortega-Rodríguez et al.[24] estimated the intermolecular interaction energy for an asphaltene-like molecule to be near −31 kcal/mol in a vacuum by using MM. From the potential profiles, analytical spherical potentials were fitted for asphaltenes and resins and the radial distribution function $g(r)$ for asphaltene was obtained from the coarse-grained simulations where the solvents were considered as uniform static background fields represented by their dielectric constants. The free energy of association was estimated to be −9 kJ/mol in both heptane and toluene, and less than −1 kJ/mol in pyridine. In another study, Stoyanov et al.[25] used three structures proposed by Takanohashi et al.[26] to calculate the interaction energies between asphaltene molecules in aggregates. They applied 3D-RISM method[27] to model the solvent effects and calculate the potential of mean force (PMF) along specific paths of asphaltene dissociation in quinoline and 1-methylnaphthalene. Their results showed different interaction energies for different dimer configurations; however, the effect of temperature on asphaltene disaggregation in solvents was not conclusive. An important issue that was not addressed in their study was the huge energy barrier (up to 20 kcal/mol) observed in the PMF profile, which would suggest that asphaltene aggregation could not occur at ambient conditions. By applying the DFT method along with 3D-RISM-KH molecular theory of solvation, da Costa et al.[28,29] calculated the free energy of dimerization for asphaltene-like molecules in dry and water-saturated chloroform as well as pure water solvents. The Gibbs free energies of dimerization in dry chloroform varied in the range of −13 to −103 kJ/mol. Furthermore, the presence of water molecules improved the stability of dimers by forming hydrogen bonds with the nitrogen atom of asphaltene molecules. Recently, Headen et al.[30] performed molecular dynamics (MD) simulations on asphaltene model molecules in explicit solvents such as heptane and toluene. They used GROMACS simulation software with OPLS-AA FF to run two types of simulations. First they considered six asphaltene molecules in the solvent with 7 wt% concentration, let the simulation proceed for 20 ns, and calculate the PMF function from $g(r)$. The second type of simulation was performed for two asphaltene molecules in a box of solvent molecules. The molecules were restrained at specific distances from 0.5 to 1.5 nm with an interval of 1 Å. The force needed to keep molecules at a specific distance was determined and the PMF profile was calculated along the distance between the COM of two molecules. The free energies of association obtained from the PMF profiles were in the range of −6 to −12 kJ/mol. The results show similar free energies of association in heptane and toluene from both methods.

In addition to the dimerization energy, asphaltene aggregation behavior has been investigated by molecular simulations in the past decade. Pacheco-Sánchez et al.[31] ran simulations on 35 asphaltene molecules with five different structures using the COMPASS98-02 FF[18] in a vacuum. They found that asphaltenes could aggregate in three different orientations (parallel stacking, offset stacking, and T-shape) and that asphaltene aliphatic side chains could reduce the size of aggregates. Takanohashi et al.[32] used MD simulations to investigate the stability of asphaltene aggregates of three model molecules at high temperatures and observed that aliphatic side chains and heteroatom functional groups contribute to the stability of trimers. Takanohashi et al.[32] also ran MD simulations on 3 different asphaltene aggregates surrounded by 30 solvent molecules to examine the effect of solvent on aggregate dissociation and surprisingly found that decalin is a better solvent for asphaltene dissociation than 1-methylnaphthalene. In another MD study, Carauta et al.[33] investigated the stability of asphaltene dimers in different solvents by measuring

the distance between their aromatic cores. The authors found that the most stable dimers (i.e., dimers with the smallest distance between their molecular cores) were in heptane whereas the least stable ones were in toluene. Moreover, asphaltene aggregation was less stable in normal butane and isobutane than in heptane. Recently Headen et al. performed MD simulations with six asphaltenes in supercritical carbon dioxide (sc-CO_2). Their findings indicate that asphaltenes have a higher tendency to aggregate in sc-CO_2 than in toluene and heptane.[30,34] Addition of limonene, which is an asphaltene inhibitor, reduced the aggregation of asphaltene substantially.

The majority of MD simulations on asphaltene aggregation in solvents have focused on the stability of dimers and trimers in a system containing six asphaltene molecules or less. Moreover, the lack of accurate and consistent data on the association free energy of asphaltenes in solvents has prompted us to conduct a comprehensive study on the subject using advanced computational resources. Therefore, the objective of this work is two-fold. Our first goal is to determine the free energy of dimerization for asphaltene model molecules in explicit solvents using the umbrella sampling technique, which is one of the most popular and reliable methods to compute PMF along any given reaction coordinate. To the best of our knowledge this method has never been used for asphaltene association. For this purpose, we have developed eight model molecules to cover van der Waals (VDW) and electrostatic interactions as well as H-bonding. The second goal is to shed light on the molecular parameters controlling the aggregation of asphaltenes by running MD simulations with 36 molecules in heptane and toluene solvents and investigating the effect of various parameters on their average aggregation number. The data obtained in this work can provide important input to statistical thermodynamic models dealing with asphaltene association and precipitation.

2. METHODS

In this study, MD simulations were performed using the GROMACS 4.5.5 simulation package and the OPLS-AA FF.[35−37] The OPLS-AA FF has been developed for organic liquids and is able to reproduce the enthalpy and density of aromatic components such as pyridine and 1-methylnaphthalene.[30,36,38] Three different types of simulations were performed to study the association of asphaltenes and their aggregation behavior. (1) The free energy of dimerization (association) of asphaltene molecules in an explicit solvent was first obtained by umbrella sampling technique (see section 2.1). (2) The interaction potential of asphaltene dimers was calculated in a vacuum to understand the relation between asphaltene intermolecular forces and their dimerization free energies (see section 2.2). (3) MD simulations were performed on 36 asphaltene model structures to monitor their aggregation behavior in heptane and toluene solvents (see section 2.3). In order to validate our parameter values, we first conducted MD simulations for 1-methylnaphthalene at ambient conditions. The calculated enthalpy of evaporation and density of this chemical compared very well with experimental values,[39] as shown in Table 1.

In MD simulations with asphaltenes, we started with the molecular structure provided by Headen and co-workers,[30,34] which is shown in Figure 1 as A01. This model molecule has a molecular weight of 712 g/mol and an aromaticity factor of 0.54. Aromaticity or aromaticity factor (f_a) is defined as the ratio of the number of aromatic carbons to the total number of

Table 1. Enthalpy of Vaporization and Liquid Density of 1-Methylnaphthalene

	experiment[33]	NPT simulation
enthalpy of vaporization (kJ/mol)	57.5	59.1
liquid density (g/L)	1001	1020

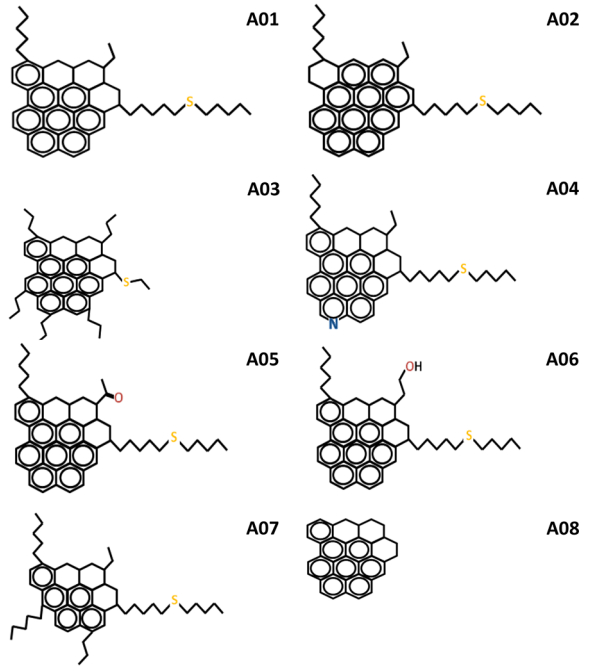

Figure 1. Structure of asphaltene-like molecules used in this study.

carbons and can be readily measured by ^{13}C NMR. Typical values of f_a range from 0.35 to 0.65 for different asphaltenes.[40−46] The polynuclear aromatic core of asphaltenes consists of eight fused aromatic rings which is in range of 4−10 aromatic rings suggested by Mullins et al.[1] To analyze the dependency of asphaltene association free energy on its molecular structure, we used seven new models (A02 to A08) derived from A01, as shown in Figure 1. All the molecular structures are similar to asphaltene structures proposed in previous works[14,20,24−26,30−34] and were optimized prior to MD simulations by using the steepest descent method in order to achieve energy minimization.

2.1. Umbrella Sampling. *2.1.1. Theory.* The PMF is an effective tool to calculate the effective interactions between two complex molecules inside a liquid medium. A routine method to compute PMF along a given reaction coordinate is umbrella sampling,[47] in which separate simulations are run along the reaction coordinate ξ, biased by umbrella potentials $w_i(\xi)$, as shown in eq 1, where ξ_i^c is the position at which the system is restrained with a force constant K_i.

$$w_i(\xi) = \frac{K_i}{2}(\xi - \xi_i^c)^2 \quad (1)$$

Since there has not been any systematic study on the umbrella force constant of asphaltene-like molecules in the past, we ran three sets of simulations for one of our molecules with force constants of 500, 1000, and 2000 kJ/(mol·nm^2), and found that 1000 kJ/(mol·nm^2) presented optimum results considering the statistical error and computational cost. The PMF can be calculated from unbiased probability distributions

dx.doi.org/10.1021/jp401584u | J. Phys. Chem. B 2013, 117, 5765−5776

Table 2. Structural Parameters of Asphaltene Model Molecules

	dipole moment (debye)	no. of aromatic carbons	no. of aliphatic carbons	heteroatoms	no. of hydrogen	aromaticity	H/C	M_w (g/mol)
A01	2.70	28	24	S	56	0.54	1.077	712
A02	2.37	32	20	S	52	0.62	1	708
A03	1.99	28	24	S	56	0.54	1.077	712
A04	4.70	27	24	N, S	55	0.53	1.078	713
A05	3.60	28	24	O, S	54	0.54	1.038	726
A06	3.16	28	24	O, S	56	0.54	1.077	728
A07	2.25	20	32	S	70	0.38	1.35	726
A08	1.98	28	7	none	22	0.80	0.63	442

of the system through eq 2, where ξ_0 is an arbitrary point where the PMF is zero.

$$W(\xi) = -k_B T \ln\left(\frac{P(\xi)}{P(\xi_0)}\right) \quad (2)$$

The unbiased probability distributions were obtained from the Weighted Histogram Analysis Method (WHAM)[48−50] implemented in the GROMACS simulation package. For statistical error calculations, we used Bayesian bootstrapping of complete histograms provided by g_wham program in GROMACS. It has been shown that Bayesian bootstrapping can accurately estimate the standard deviation function of PMF from umbrella sampling.[49]

2.1.2. Dimerization Free Energy. To calculate the free energy of dimerization in explicit solvents, we need to obtain the PMF profile of two asphaltene molecules versus their COM distance. To generate the initial configurations for each umbrella window simulation, we pulled the COM of one of the asphaltene molecules along the *Z*-axis while restraining the COM of the other one, with the pull code implemented in GROMACS package, at the rate of 2.6 nm/ns. During the pulling and window simulations, only one atom of one of the molecules was constrained so that the two molecules would be able to rotate and assume any configuration that is energetically favorable. The space between two consecutive distances is at most 0.5 Å; however, tighter spacing was used in some areas. For each initial configuration, NPT simulation was run for 300 ps to bring the system into the equilibrium temperature and pressure. The average temperature and pressure were checked at the end of NPT simulations to make sure the system was equilibrated. The window simulations lasted for 10 ns (with a time step of 2 fs) to allow enough time for two asphaltene molecules to explore all possible configurations. During the simulations, asphaltene and solvent molecules were independently coupled with Nose-Hoover thermostat for temperature control. The Parrinello−Rahman algorithm was used for pressure coupling. Brendsen pressure coupling can provide correct average pressures but arguably does not produce the exact NPT ensembles.[51] All simulations were performed at constant temperature of 300 K and pressure of 1 bar. The particle-mesh Ewald algorithm was used to account for long range electrostatic interactions and the VDW cut off radius was set to 1 nm. Umbrella sampling simulations were conducted in a cubic box (6.25 nm × 6.25 nm × 6.25 nm) with the periodic boundary conditions.

2.2. Decomposition of Asphaltene Interaction Potentials. Finding the non-bonding interactions between two asphaltene molecules can help to understand their association behavior. Since all forces in MD are pairwise additive, the forces that two particles exert on each other would be the same in an explicit solvent and in a vacuum. To achieve the optimum configuration of asphaltene dimers and monomers, the potential energy was minimized with a force tolerance of 1 kJ/(mol·nm). Furthermore, several different initial configurations are required to ensure that the global minimum is reached. For this purpose, a snapshot of asphaltene dimers (without the solvent molecules) was taken at every 100 ps during the first three umbrella windows simulations. A total of 300 initial configurations for each asphaltene dimer was used to find the global energy minimum. For monomers, we ran MD simulations for 5 ns and generated 50 initial configurations. The non-bonding interaction potential energies during dimerization were calculated from eq 3, where the non-bonding term is the VDW or electrostatic potential.

$$E_{\text{inter(non-bonding)}} = E_{\text{dimer(non-bonding)}} - 2E_{\text{monomer(non-bonding)}} \quad (3)$$

2.3. Asphaltene Aggregation. In order to investigate the impact of dimerization free energy on the aggregation behavior of asphaltenes, we placed 36 molecules of each model asphaltene (see Figure 1) in heptane, all more than 1.5 nm from each other. For A01 asphaltene, an additional simulation was run with toluene. The concentration of asphaltenes was kept constant at 7 wt% in both heptane and toluene. To equilibrate our systems, a quick energy minimization was first run followed by 200 ps of NVT and NPT ensemble simulations to bring asphaltene and solvent molecules to the equilibrium T and P of 300 K and 1 bar, respectively. The average *T* and *P* during the NPT simulation were checked to ensure that the system was in equilibrium. The production simulations were run for 80 ns with simulation parameters similar to those described in section 2.1.2 except for VDW (where the cut off radius was set to 1.2 nm and the size of simulation box was 10 nm × 10 nm × 10 nm). At the end of MD simulations, the distance between each pair of asphaltene molecules was measured every 10 ps to determine whether they are in the aggregate state or not. Based on our criteria, aggregation occurs if the COM of two asphaltenes is less than 0.85 nm. If this distance is between 0.85 and 1.25 nm, then aggregation would be accepted or rejected on the basis of the track of their distances in the past or following time frames. Aggregation does not occur for distances higher than 1.25 nm. The results were tested for several time frames of different asphaltenes, and the method proved to be accurate in detecting the aggregation state.

3. RESULTS AND DISCUSSION

3.1. Dimerization Free Energy. The molecular structures of our model molecules were calculated and are tabulated in Table 2.

dx.doi.org/10.1021/jp401584u | J. Phys. Chem. B 2013, 117, 5765−5776

The PMF vs the distance between the COM of two A01 molecules in heptane is shown in Figure 2. All of the PMF results presented herein have been corrected for the entropy artifact that is generally inherited in umbrella sampling simulations.[52] According to this figure; the lowest energy configuration is at a distance of 5 Å. Because the two molecules are offset parallel toward each other, the distance between the centers of mass is higher than the one between aromatic planes (which is ∼3−4 Å).[1,21,31] For A01 molecule, we found the optimum distance between aromatic core planes to be ∼3 Å. Figure 2 also shows the statistical error associated with umbrella sampling calculated from the complete histogram using Bayesian bootstrap technique. The error is ∼1 kJ/mol.

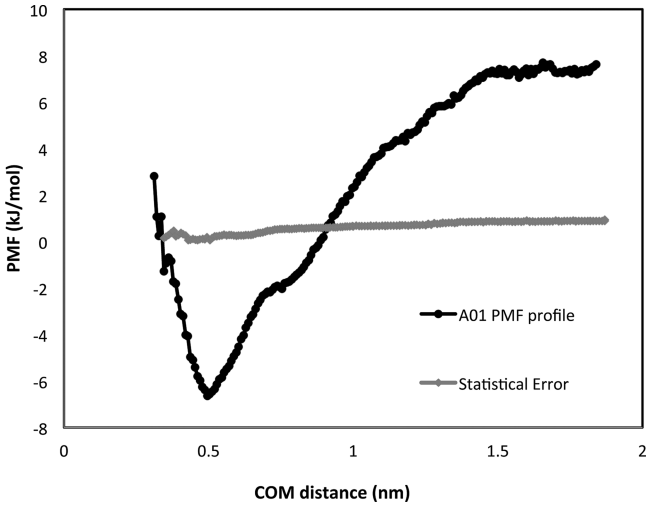

Figure 2. Potential of mean force profile and statistical error in umbrella sampling for A01 molecules in heptane.

Another feature in Figure 2 is the slight flattening of the profile between 0.7 and 0.8 nm, which corresponds to a T-shape configuration based on the simulation trajectory. The reason why a second minimum cannot be seen between 0.7 and 0.8 nm is probably because of the aliphatic side chains of asphaltene A01, which prevent the two aromatic planes from getting closer to each other in the T-shape configuration. When the aliphatic chains are removed, as in molecule A08, a second minimum can clearly be seen around 0.8 nm. It should be noted that we have repeated the A08 and A01 simulations and found identical PMF profiles. When the number and average length of aliphatic chains is increased, as in molecule A07, it becomes harder for the aromatic cores to have a T-shape configuration due to higher steric repulsion, and therefore the second minimum disappears in the PMF profile, as shown in Figure 3. Two snapshots of A08 asphaltenes (without heptane molecules) are provided in Figure 4 to depict the offset-parallel and T-shape configurations.

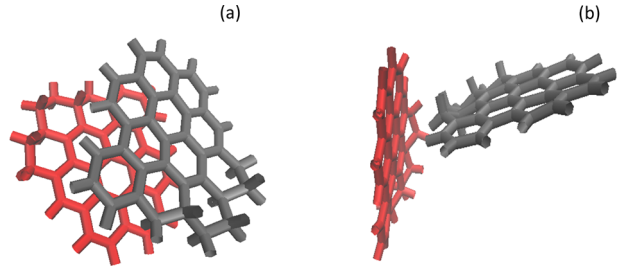

Figure 4. Snapshots of umbrella sampling simulations for A08 asphaltenes without heptane molecules to depict (a) offset parallel and (b) T-shape configurations.

The free energy of dimerization is the difference between the minimum value of PMF (at $r \approx 0.5$ nm) and the value of PMF at higher distances when it reaches a plateau ($r > 1.5$ nm). The dimerization free energies for all the molecular structures shown in Figure 1 calculated in heptane solvent, along with the value for A01 calculated in toluene, are tabulated in Table 3.

In the following we will discuss the effects of structural parameters of the molecules on the association free energy.

3.1.1. Aromatic Rings in Polynuclear Aromatic Core. Let us consider molecules A01 and A02 in Figure 1 with 8 and 11

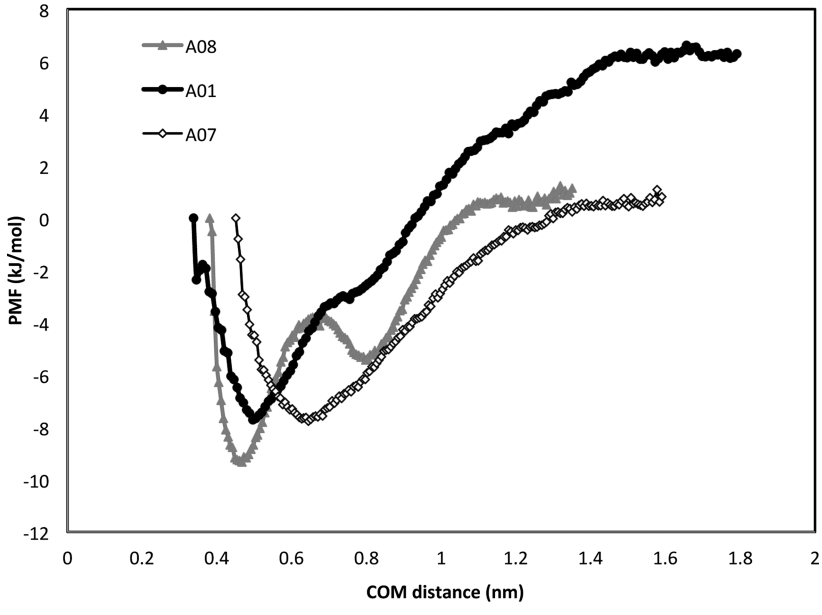

Figure 3. PMF profile for A01, A07, and A08 asphaltenes in heptane.

dx.doi.org/10.1021/jp401584u | J. Phys. Chem. B 2013, 117, 5765−5776

Table 3. Free Energy of Dimerization for Different Asphaltene Structures in Organic Solvents

molecule	solvent	free energy of dimerization (kJ/mol)
A01	toluene	−11.4
A01	heptane	−14.0
A02	heptane	−19.4
A03	heptane	−13.0
A04	heptane	−19.1
A05	heptane	−15.0
A06	heptane	−17.7
A07	heptane	−8.3
A08	heptane	−10.0

aromatic rings, respectively. To keep the molecular weight and the size of the asphaltene core constant, the three cyclic aliphatic rings were converted to aromatic rings in A02. However, it should be noted that forming 12 aromatic rings in this configuration was not possible since there cannot be double bonds between all aromatic carbons. This trivial mistake has been repeated several times in different molecular simulations of asphaltenes.[14,33,53] Based on our MD simulations, the free energies of dimerization for A01 and A02 are −14 and −19.4 kJ/mol, respectively. This shows that the association energy (absolute value) substantially increases with the increase in the number of aromatic carbons.

3.1.2. Length of Aliphatic Side Chains. To understand the effect of aliphatic side chains on the free energy of dimerization, two molecular structures were used: A01 and A03. The only difference between these two molecules is the number and length of their side chains. Asphaltene A03 has six side chains with an average length of almost 3, whereas asphaltene A01 has three side chains with an average chain length of 5.7. The propane chain in A03 was placed on site 1 instead of site 2, to prevent the repulsive interaction between two hydrogen atoms (as illustrated by a red oval in the structure shown in Figure 5).[54] This phenomenon is called the pentane effect because

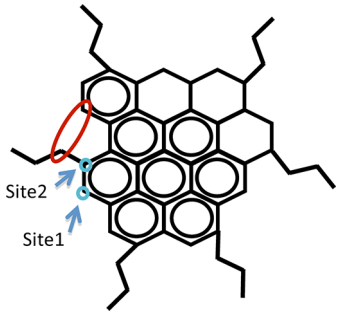

Figure 5. Asphaltene structure with pentane effect.

pentane is the smallest molecule in which it may occur. The pentane effect can cause significantly higher internal energy and nonplanarity in the aromatic core, which can lead to errors in molecular simulation.

The free energy of association for A01 and A03 asphaltenes is −14 and −13 kJ/mol, respectively, which is the same within the error bar of our simulations. Therefore, the distribution of aliphatic carbons in the side chains does not have a significant impact on the association energy of two molecules if other parameters (such as number of aromatic rings, core size, heteroatom content, and molecular weight) are kept constant.

3.1.3. Heteroatoms. Asphaltene polarity is attributed to the presence of heteroatoms (N, O, and S) and metals in its molecular structure. Since the metal content is very small, we did not consider any metals in our molecular models. Heteroatoms in asphaltenes can be found in different functional groups; nitrogen is mostly in pyridinic or pyrolic functional groups, oxygen is more abundant in phenolic, carboxylic, hydroxylic, and ketonic functional groups, and sulfur is most likely to be found in sulfuric and thiophene conformations.[55] To analyze the effect of heteroatoms on asphaltene aggregation, we considered two molecular structures: A04 and A05. In A04 one aromatic carbon was replaced with nitrogen to create pyridine functional group, and in A05 one ketonic functional group was added to one of the aliphatic chains. The purpose of choosing these two structures was to enable us to examine the effect of heteroatoms attached to both aromatic and aliphatic parts of asphaltenes. The inclusion of heteroatoms changes the polarity of asphaltene and thus its dipole moment, as seen in Table 2.

Based on our MD simulations, the free energy of A01, A05, and A04 dimerization in heptane is −14, −15, and −19.1 kJ/mol, respectively. These data indicate no apparent correlation between polarity (or heteroatom content) and the association free energy. However, heteroatoms attached to the aromatic core have a higher impact on the association strength than the ones attached to the aliphatic side chains. This is because heteroatoms attached to aromatic rings can affect the strength of aromatic interactions by changing the π electron cloud density. For large aromatic moieties, the optimum dimer configuration is (offset) parallel stacking since it provides better overlap between the large planar surfaces and hence stronger VDW attraction. Although in this configuration there is also an electrostatic repulsion between the surfaces due to the electron clouds, the repulsion has a smaller magnitude than the VDW attraction. This could be the reason why the offset parallel configuration becomes more favorable than the T-shape one when the size of aromatic core increases. As a consequence, asphaltenes with large aromatic cores prefer the face-to-face stacking over the T structure, which is opposite, e.g., to benzene dimers. Nitrogen is an electron-withdrawing substituent meaning that substitution of aromatic carbon with nitrogen reduces the size of π electron clouds and this electron deficiency in π-system results in lower electrostatic repulsion between the electron clouds and more stable parallel stacking of dimers.[11,12] Table 4 compares the VDW (LJ forces) and the

Table 4. Interaction Energies (in kJ/mol) between Two Asphaltene Molecules in a Vacuum

	ΔG of dimerization	Lennard-Jones potential	Coulomb potential	total interaction potential
A01	−14	−177.5	4.6	−172.9
A04	−19.1	−179.3	−0.2	−179.6
A06	−17.7	−165.2	−37.9	−203.2

electrostatic (coulomb forces) contributions to the potential energy of A01, A04, and A06 asphaltene dimers in a vacuum. According to this table, the main interaction is the VDW attraction between molecules. As expected, the addition of nitrogen atom to A01 (as in A04) has lowered the electrostatic repulsion to almost zero. The electrostatic contribution of A06 is mainly due to hydrogen bonding and will be discussed in the next section.

dx.doi.org/10.1021/jp401584u | J. Phys. Chem. B 2013, 117, 5765−5776

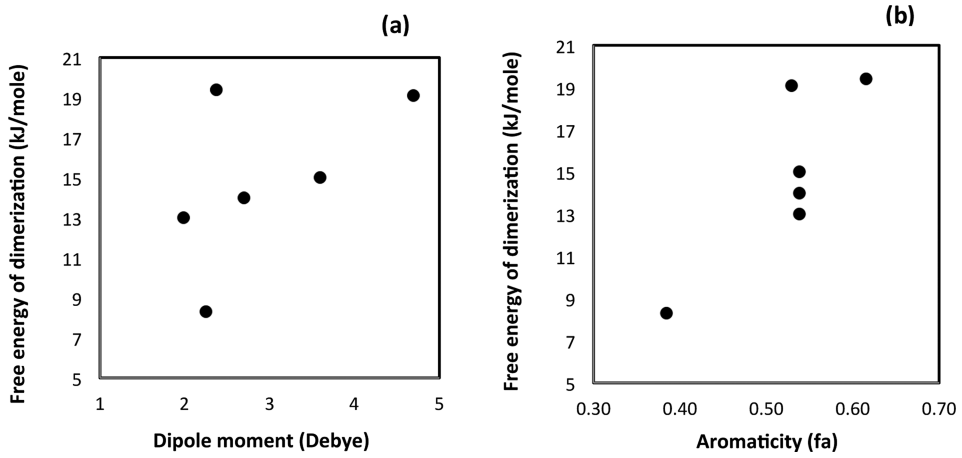

Figure 6. (a) Gibbs free energy of dimerization vs dipole moment of asphaltene molecules. (b) Gibbs free energy of dimerization vs aromaticity of asphaltene molecules.

It should be mentioned that, although in our molecular simulations we did not deal with the π electron cloud explicitly, the effect of nitrogen on aromatic interactions was considered through the partial charges that were obtained from the quantum calculations on the quinoline molecule. We have optimized A04 at the Hartree−Fock level of theory with 6-31G(d) basis set and found the ChelpG partial charges for N and the surrounding carbons in agreement with the OPLS partial charges provided for quinoline.

3.1.4. Hydrogen-Bonding. To assess the contribution of H-bonding, one hydroxyl group was added to the side aliphatic chain of A01 to create A06 molecule, as shown in Figure 1. In a vacuum, this addition has resulted in a slightly lower VDW attraction between aromatic cores and a much larger electrostatic attraction due to H-bonding between hydroxyl groups in aliphatic chains, as indicated in Table 4. However, based on US simulations in heptane, the free energy of association for A06 molecule was −17.7 kJ/mol and has increased in magnitude merely by 3.7 kJ/mol, compared to A01 molecule. Therefore, H-bonding is not the main mechanism of association between asphaltene even though it can help to produce stronger dimers.

3.1.5. Solvent. Toluene and heptane represent two end points of the solvent spectrum for asphaltenes. Indeed, toluene is known as a good solvent for asphaltenes; however, heptane is the API standard precipitant of asphaltene. If the main interaction between asphaltenes is the aromatic interaction, then one expects the dimerization free energy to be different in toluene than in heptane. Unlike heptane, the benzene ring in toluene can interact with asphaltene aromatic cores through aromatic interactions. Although heptane and toluene have similar molecular weights (100 and 92 g/mol) and dielectric constants (1.92 and 2.38, respectively), and both are nonpolar molecules (with dipole moments of 0 and 0.36 D, respectively), they should not be represented implicitly as a background field to model asphaltene aggregation because similar results are bound to be obtained.[24]

Based on more than 70 umbrella window simulations, the free energy of association for A01 asphaltene in heptane and toluene is −14 and −11.4 kJ/mol, respectively (see Table 3). These data confirm that asphaltenes have a smaller tendency to aggregate in toluene than in heptane. This is probably due to the fact that the benzene ring of toluene can have aromatic interactions with the core of asphaltenes, which would lead to a lower free energy of association in absolute value. The results for A01 asphaltene in heptane and toluene are very well in the range of association energies obtained by Headen et al.[30] using a different algorithm. However, our simulations were able to capture the difference in dimerization free energy of asphaltenes in heptane and toluene solvents.

3.1.6. Aromaticity vs Polarity. There has been a long debate on the role of polarity and aromaticity on asphaltene aggregation. Because asphaltenes from unstable oils and field deposits are generally more polar and aromatic than asphaltenes from stable oils,[56,57] polarity and/or aromaticity are believed to be responsible for the instability of asphaltenes in crude oils. However, a recent study by Sedghi and Goual[58] suggested that asphaltene aggregation is mainly driven by their aromaticity rather than polarity. This is in agreement with the data presented in Figure 6, where a trend is observed between the free energy of dimerization and aromaticity but not the dipole moment. Furthermore, Figure 6 and Table 2 reveal that A02 and A04 molecules have similar energies of dimerization, even though A04 is less aromatic than A02. This is due to the presence of nitrogen in the aromatic core of A04, which increases the aromatic interactions between two asphaltenes. Therefore, it is the strength of $\pi-\pi$ aromatic interactions between asphaltene cores rather than their aromaticity that should be considered as the driving force for association.

3.1.7. Free Energy of Association for Trimers. For A01 asphaltene molecules, the free energy of association between a monomer and a dimer to form a trimer was found to be −21 kJ/mol, which is 50% higher than the association free energy between two monomers. This shows that the far end molecules in a trimer can interact with each other and although their attractions are smaller than the ones between neighboring molecules, they can have a noticeable contribution to the stability of trimers.

3.2. Average Aggregation Number. The aggregation behavior of asphaltenes may not follow the same trend as the dimerization of two molecules since the accessibility of association sites may become more important during aggregation than dimerization. In particular, the role of aliphatic side chains during dimerization and aggregation can be different. Table 3 reveals that the removal of all aliphatic chains (as shown in A08 molecule) decreased the dimerization free energy (absolute value) by 3−4 kJ/mol. This is in line with the results of Takanohashi et al.,[26] who found that aliphatic chains contribute to the stability of trimers. To study this effect

dx.doi.org/10.1021/jp401584u | J. Phys. Chem. B 2013, 117, 5765−5776

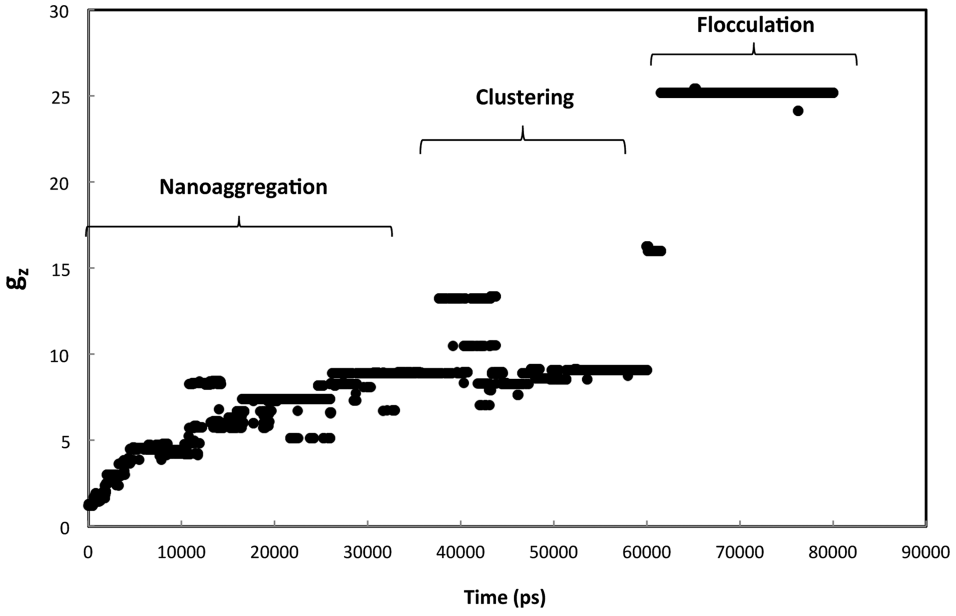

Figure 7. Average aggregation number (g_z) during MD simulation of A04 asphaltenes in heptane.

on larger asphaltene aggregates, 36 molecules of each model in Figure 1 were inserted in heptane at 7 wt% concentration. The simulations were run for 80 ns at the equilibrium pressure and temperature of 1 bar and 300 K, respectively. The *z*-average aggregation number, g_z, was calculated from eq 4, where n_i is the number of aggregates i containing g_i monomers.[59]

$$g_z = \frac{\sum_i n_i g_i^3}{\sum_i n_i g_i^2} \tag{4}$$

Figure 7 shows the aggregation number of A04 asphaltenes during MD simulations in heptane. The aggregation of asphaltenes can be divided into three stages: (1) In the first stage, asphaltene molecules start to form nanoaggregates with g_z = 8−10 (4−11 monomers per nanoaggregate). (2) In the second stage, 2−3 nanoaggregates start to form a large cluster, and g_z increases to 14−16. (3) In the final stage, other nanoaggregates join the cluster, and asphaltenes flocculate or precipitate with g_z > 25.

Figure 8 shows a snapshot of 36 molecules of A04 asphaltene forming one large cluster after 80 ns of MD simulation in heptane. For the purpose of clarity, we removed the heptane molecules from this Figure. The same behavior has been observed for A02, A06, and A08 asphaltenes. The top panel of Figure 9 depicts the average aggregation numbers of A02 and A06 molecules. The simulation trajectories (or movies) for A01 and A05 asphaltenes show that while they can form a cluster, the cluster is not stable enough to flocculate, as the nanoaggregates attach and detach continuously. Note that a similar behavior was observed for A01 asphaltenes in toluene with a very unstable cluster. In heptane, asphaltenes A03 and A07 cannot form clusters, and their aggregation remains at the nanoaggregation stage. The bottom panel of Figure 9 compares the average aggregation number for A01 and A03 asphaltenes.

3.2.1. Modified Yen Model. Our simulations show that asphaltenes with higher (or more negative) dimerization free energy start to form nanoaggregates consisting of 4−11 molecules with an average aggregation number of 8−10. After nanoaggregates are formed, they start to move slowly toward each other and create larger aggregates or clusters. With the exception of A08 molecules, asphaltenes with strong association energy form stable clusters that precipitate. This is the first MD simulation study that could verify the modified Yen or Yen−Mullins model.

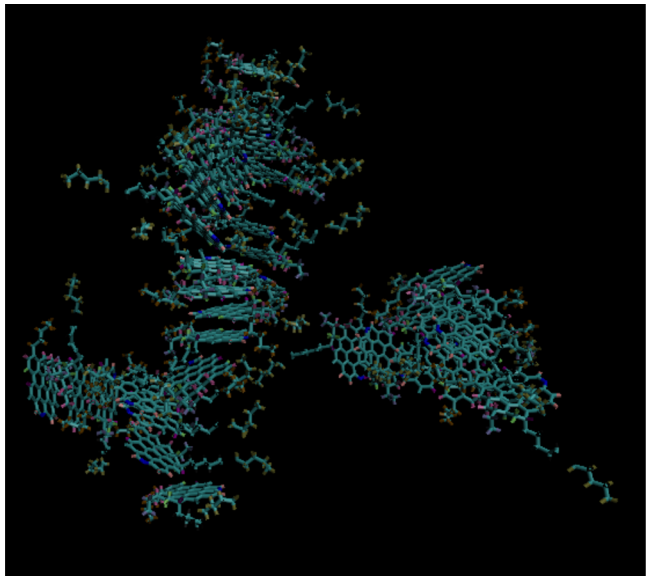

Figure 8. Flocculation state of A04 asphaltenes after 80 ns of MD simulation in heptane.

3.2.2. Forces Limiting Aggregation. According to the modified Yen model, the forces limiting asphaltene aggregation stem from the steric repulsion between aliphatic side chains. In this study, we attempted to test this concept by monitoring the aggregation behavior of two asphaltenes with different aliphatic chain structures (A01 and A03) and one asphaltene without any aliphatic chains (A08). According to Figure 9 (bottom), there is a remarkable difference between the aggregate size of A01 and A03 asphaltenes as the latter has a much less tendency to aggregate than the former. Considering that the dimerization free energies of A01 and A03 are similar (see Table 3), the difference in their aggregation behavior is related to their

dx.doi.org/10.1021/jp401584u | J. Phys. Chem. B 2013, 117, 5765−5776

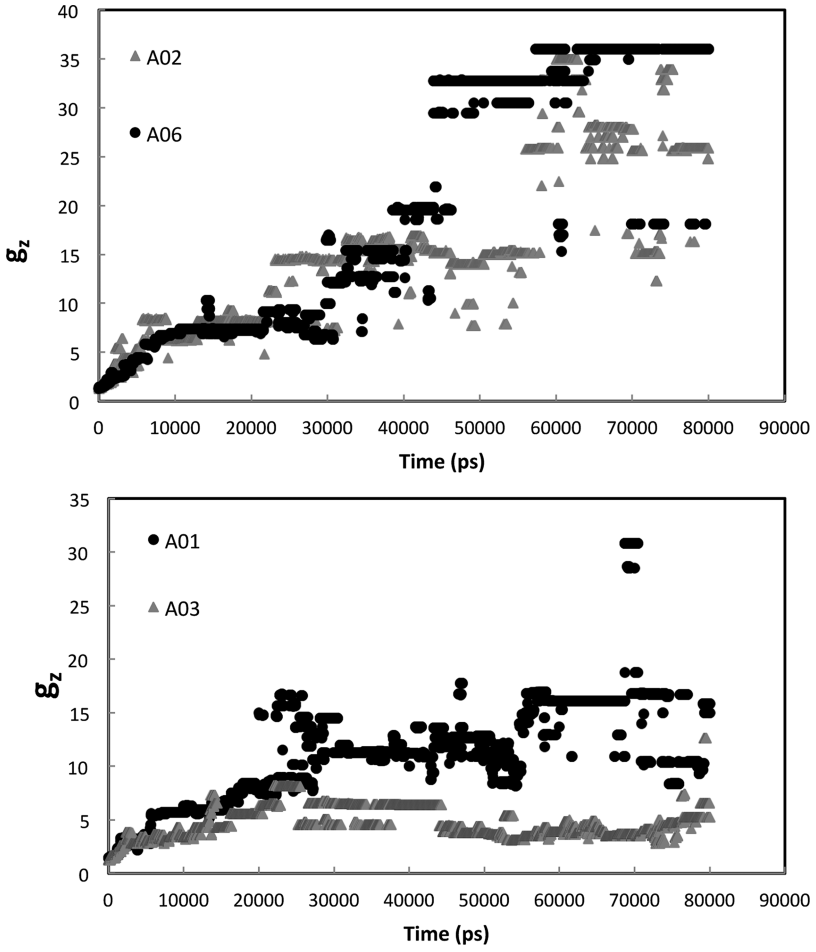

Figure 9. Average aggregation numbers for A01, A02, A03, and A06 asphaltenes in heptane.

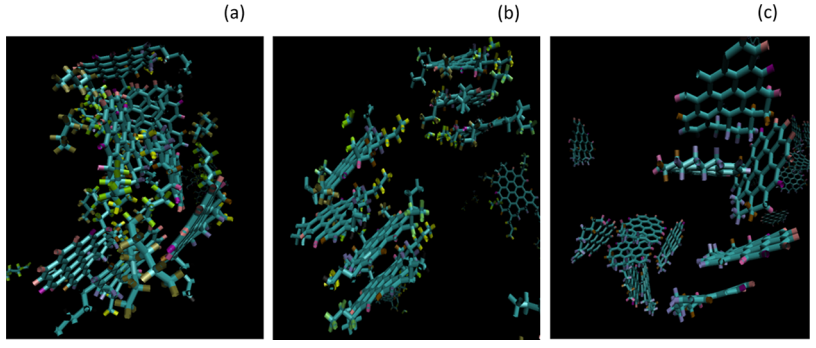

Figure 10. Average nanoaggregate structure for three asphaltenes in heptane: (a) A01, (b) A03, and (c) A08.

different aliphatic chain structures. The MD movies of these two asphaltenes showed that A03 molecules can only form nanoaggregates with parallel configuration whereas A01 molecules can form nanoaggregates with both parallel and T-shape configurations, as clearly shown in Figure 10a,b. The fact that A03 molecules cannot form T-shape configurations severely limits the accessibility of association sites (aromatic cores) to two sites per nanoaggregate (i.e., two heads of the cylinder-shaped stack). In this case, nanoaggregates cannot grow beyond 4−5 molecules. This observation is in accord with umbrella sampling simulations where the PMF profile of A03 asphaltene was similar to A07 asphaltene in Figure 3, indicating that A03 dimers do not have any T-shape configuration due to steric repulsions between aliphatic chains of one molecule and the aromatic core of another molecule.

The T-shape configuration is predominant in nanoaggregates of A08 asphaltene (see Figure 10c) due to the absence of aliphatic side chains. Although A08 molecules form smaller nanoaggregates than A01 molecules (due to smaller molecular weight and hence smaller ΔG of dimerization), they form more stable clusters that flocculate, as there are no steric repulsions between nanoaggregates. This is in accord with the work of Pacheco-Sánchez et al.,[29] who found that the presence of aliphatic chains reduces the size of asphaltene aggregates.

3.2.3. Hydrogen-Bonding. In section 3.1.4, we showed that the presence of hydroxyl groups in aliphatic side chains did not significantly affect the dimerization free energy of A06

dx.doi.org/10.1021/jp401584u | J. Phys. Chem. B 2013, 117, 5765−5776

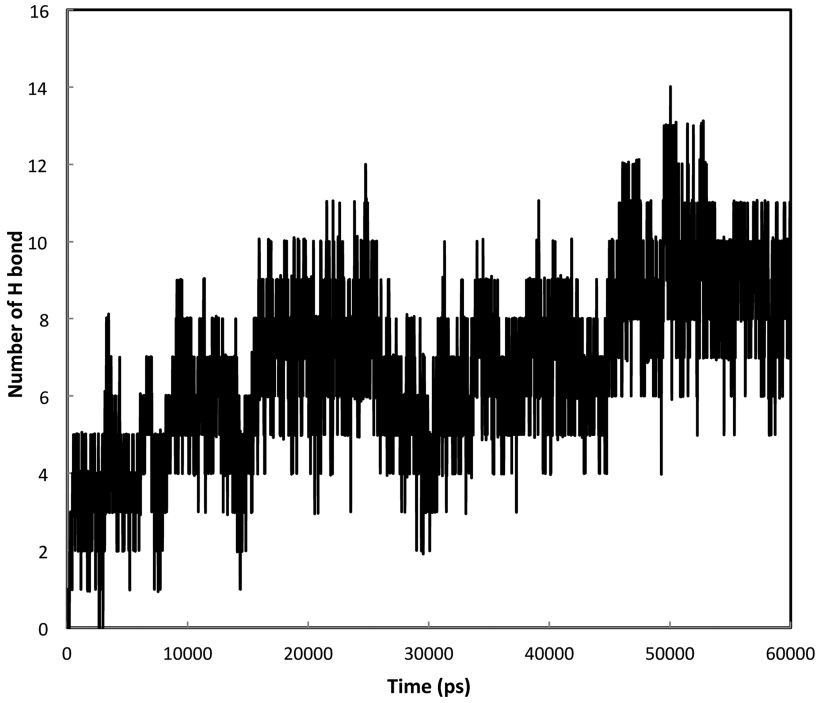

Figure 11. Number of hydrogen bonds between A06 asphaltene molecules in heptane.

asphaltenes. In this section, we investigate the effect of H-bonding on asphaltene aggregation. During the simulation of 36 molecules of A06 asphaltenes, we were able to identify as many as 14 hydrogen bonds between molecules based on the distance between the hydroxyl groups. Figure 11 shows that the average number of hydrogen bonds is between 7 and 10. The MD trajectories suggest that A06 asphaltenes have a stronger aggregation tendency than A02 and A04 asphaltenes even though their dimerization free energy is smaller. This could be attributed to H-bonding which may constitute a second association site for asphaltenes when accessibility to aromatic cores becomes harder in larger aggregates.

4. CONCLUSIONS

In this study, the umbrella sampling method has been successfully applied to calculate asphaltene dimerization free energies in explicit solvents such as toluene and heptane. The results suggest that the strength of aromatic interactions between asphaltene aromatic cores is the driving force for association. This strength is dependent not only on the number of aromatic rings but also on the presence of heteroatoms in the aromatic core that can reduce the electrostatic repulsion. The association free energy of asphaltene is higher (or more negative) in heptane than in toluene due to aromatic interactions between toluene and asphaltene molecules. The size and number of aliphatic side chains have little effect on the dimerization of asphaltenes; however, their impact on aggregation can be prominent due to the steric repulsion caused by aliphatic side chains. Similarly, H-bonding has more effect on aggregation than dimerization as it provides a second association site in large aggregates.

The MD simulation of 36 asphaltene molecules in heptane are in agreement with the modified Yen model and manifests three stages of aggregation: nanoaggregation (g_z = 8−10), clustering (g_z = 14−16), and flocculation (g_z > 25). Flocculation was observed for asphaltenes with higher association free energy (A02, A04, and A06) and without aliphatic side chains (A08). Asphaltenes with moderate association strength (A01 and A05) formed a cluster that did not flocculate whereas asphaltenes with the weakest association strength (A07) remained in the nanoaggregate stage. Although A01 and A03 asphaltenes have a similar free energy of association, they show a different aggregation tendency. This is because A03 molecules cannot form T-shape configuration due to the steric repulsion between the six short aliphatic chains and the aromatic core, and this severely limits the accessibility of the association sites to the two ends of the aggregate.

AUTHOR INFORMATION

Corresponding Author

*E-mail: lgoual@uwyo.edu. Phone: +1 307 766 3278.

Notes

The authors declare no competing financial interest.

ACKNOWLEDGMENTS

This work was supported in part by a National Science Foundation CAREER 0846140 grant (to J.K.).

REFERENCES

(1) Mullins, O. C. The Modified Yen Model. *Energy Fuels* **2010**, *24*, 2179−2207.

(2) Mullins, O. C.; Sabbah, H.; Eyssautier, J.; Pomerantz, A. E.; Barré, L.; Andrews, A. B.; Ruiz-Morales, Y.; Mostowfi, F.; McFarlane, R.; Goual, L.; et al. Advances in Asphaltene Science and the Yen−Mullins Model. *Energy Fuels* **2012**, *26*, 3986−4003.

(3) Carauta, A. N. M.; Correia, J. C. G.; Seidl, P. R.; Silva, D. M. Conformational Search and Dimerization Study of Average Structures of Asphaltenes. *J. Mol. Struct. (Theochem)* **2005**, *755*, 1−8.

(4) Speight, J. G. *The Chemistry and Technology of Petroleum*; Marcel Dekker: New York, 1999; Chapter 11.

(5) Taylor, S. E. Use of Surface Tension Measurements to Evaluate Aggregation of Asphaltenes in Organic Solvents. *Fuel* **1992**, *71*, 1338−1339.

(6) Ting, P. D.; Hirasaki, G. J.; Chapman, W. G. Modeling of Asphaltene Phase Behavior with the SAFT Equation of State. *Pet. Sci. Technol.* **2003**, *21*, 647−661.
(7) Gonzalez, D. L.; Hirasaki, G.; Chapman, W. G. Prediction of Asphaltene Instability under Gas Injection with the PC-SAFT Equation of State. *Energy Fuels* **2005**, *19*, 1230−1234.
(8) Gonzalez, D. L.; Hirasaki, G. J.; Creek, J.; Chapman, W. G. Modeling of Asphaltene Precipitation Due to Changes in Composition Using the Perturbed Chain Statistical Associating Fluid Theory Equation of State. *Energy Fuels* **2007**, *21*, 1231−1242.
(9) Li, Z.; Firoozabadi, A. Modeling Asphaltene Precipitation by n-Alkanes from Heavy Oils and Bitumens Using Cubic-Plus-Association Equation of State. *Energy Fuels* **2010**, *24*, 1106−1113.
(10) Li, Z.; Firoozabadi, A. Cubic-Plus-Association Equation of State for Asphaltene Precipitation in Live Oils. *Energy Fuels* **2010**, *24*, 2956−2963.
(11) Hunter, C. A.; Lawson, K. R.; Perkins, J.; Urch, C. J. Aromatic interactions. *J. Chem. Soc., Perkin Trans. 2* **2001**, *0*, 651−669.
(12) Hunter, C. A.; Sanders, J. K. M. The Nature of π-π Interactions. *J. Am. Chem. Soc.* **1990**, *112*, 5525−5534.
(13) Rodríguez, J.; Sanchez-Marin, J.; Torrens, F.; Ruette, F. Molecular Aggregation of Polycyclic Aromatic Hydrocarbons. A Theoretical Modelling of Coronene Aggregation. *J. Mol. Struct. (Theochem)* **1992**, *254*, 429−441.
(14) Rogel, E. Simulation of Interactions in Asphaltene Aggregates. *Energy Fuels* **2000**, *14*, 566−574.
(15) Hagler, A. T.; Huler, E.; Lifson, S. Energy Functions for Peptides and Proteins. I. Derivation of a Consistent Force Field Including the Hydrogen Bond from Amide Crystals. *J. Am. Chem. Soc.* **1974**, *96*, 5319−5327.
(16) Sun, H.; Rigby, D. Polysiloxanes: ab Initio Force Field and Structural, Conformational and Thermophysical Properties. *Spectrochim. Acta A* **1997**, *53*, 1301−1323.
(17) Rigby, D.; Sun, H.; Eichinger, B. E. Computer Simulations of Poly(Ethylene Oxide): Force Field, PVT Diagram and Cyclization Behaviour. *Polym. Int.* **1997**, *44*, 311−330.
(18) Sun, H.; Ren, P.; Fried, J. R. The COMPASS Force Field: Parameterization and Validation for Phosphazenes. *Comput. Theor. Polym. Sci.* **1998**, *8*, 229−246.
(19) Sun, H. COMPASS: An ab Initio Force-Field Optimized for Condensed-Phase Applications−Overview with Details on Alkane and Benzene Compounds. *J. Phys. Chem. B* **1998**, *102*, 7338−7364.
(20) Pacheco-Sánchez, J. H.; Zaragoza, I. P.; Martínez-Magadán, J. M. Asphaltene Aggregation under Vacuum at Different Temperatures by Molecular Dynamics. *Energy Fuels* **2003**, *17*, 1346−1355.
(21) Alvarez-Ramirez, F.; Ramirez-Jaramillo, E.; Ruiz-Morales, Y. Calculation of the Interaction Potential Curve between Asphaltene−Asphaltene, Asphaltene−Resin, and Resin−Resin Systems Using Density Functional Theory. *Energy Fuels* **2006**, *20*, 195−204.
(22) Harris, J. Simplified Method for Calculating the Energy of Weakly Interacting Fragments. *Phys. Rev. B* **1985**, *31*, 1770−1779.
(23) Perdew, J. P.; Wang, Y. Accurate and Simple Analytic Representation of the Electron-Gas Correlation Energy. *Phys. Rev. B* **1992**, *45*, 13244−13249.
(24) Ortega-Rodríguez, A.; Cruz, S. A.; Gil-Villegas, A.; Guevara-Rodríguez, F.; Lira-Galeana, C. Molecular View of the Asphaltene Aggregation Behavior in Asphaltene-Resin Mixtures. *Energy Fuels* **2003**, *17*, 1100−1108.
(25) Stoyanov, S. R.; Gusarov, S.; Kovalenko, A. Multiscale Modelling of Asphaltene Disaggregation. *Mol. Simul.* **2008**, *34*, 953−960.
(26) Takanohashi, T.; Sato, S.; Saito, I.; Tanaka, R. Molecular Dynamics Simulation of the Heat-Induced Relaxation of Asphaltene Aggregates. *Energy Fuels* **2003**, *17*, 135−139.
(27) *Understanding Chemical Reactivity: Molecular Theory of Solvation*; Hirata, F., Ed.; Kluwer Academic Publishers, New York, 2003; Vol. *24*, pp 169−275.
(28) da Costa, L. M.; Stoyanov, S. R.; Gusarov, S.; Tan, X.; Gray, M. R.; Stryker, J. M.; Tykwinski, R.; Carneiro, J. W. M.; Seidl, P. R.; Kovalenko, A. Density Functional Theory Investigation of the Contributions of π−π Stacking and Hydrogen-Bonding Interactions to the Aggregation of Model Asphaltene Compounds. *Energy Fuels* **2012**, *26*, 2727−2735.
(29) da Costa, L. M.; Hayaki, S.; Stoyanov, S. R.; Gusarov, S.; Tan, X.; Gray, M. R.; Stryker, J. M.; Tykwinski, R.; Carneiro, W. M. J.; Sato, H.; et al. 3D-RISM-KH Molecular Theory of Solvation and Density Functional Theory Investigation of the Role of Water in the Aggregation of Model Asphaltenes. *Phys. Chem. Chem. Phys.* **2012**, *14*, 3922−3934.
(30) Headen, T. F.; Boek, E. S.; Skipper, N. T. Evidence for Asphaltene Nanoaggregation in Toluene and Heptane from Molecular Dynamics Simulations. *Energy Fuels* **2009**, *23*, 1220−1229.
(31) Pacheco-Sánchez, J. H.; Álvarez-Ramírez, F.; Martínez-Magadán, J. M. Morphology of Aggregated Asphaltene Structural Models. *Energy Fuels* **2004**, *18*, 1676−1686.
(32) Takanohashi, T.; Sato, S.; Tanaka, R. Structural Relaxation Behaviors of Three Different Asphaltenes Using MD Calculations. *Pet. Sci. Technol.* **2004**, *22*, 901−914.
(33) Carauta, A. N. M.; Seidl, P. R.; Chrisman, E. C. A. N.; Correia, J. C. G.; Menechini, P. O.; Silva, D. M.; Leal, K. Z.; de Menezes, S. M. C.; de Souza, W. F.; Teixeira, M. A. G. Modeling Solvent Effects on Asphaltene Dimers. *Energy Fuels* **2005**, *19*, 1245−1251.
(34) Headen, T. F.; Boek, E. S. Molecular Dynamics Simulations of Asphaltene Aggregation in Supercritical Carbon Dioxide with and without Limonene. *Energy Fuels* **2011**, *25*, 503−508.
(35) Jorgensen, W. L.; Maxwell, D. S.; Tirado-Rives, J. Development and Testing of the OPLS All-Atom Force Field on Conformational Energetics and Properties of Organic Liquids. *J. Am. Chem. Soc.* **1996**, *118*, 11225−11236.
(36) Jorgensen, W. L.; Laird, E. R.; Nguyen, T. B.; Tirado-Rive, J. Monte Carlo Simulations of Pure Liquid Substituted Benzenes with OPLS Potential Functions. *J. Comput. Chem.* **1993**, *14*, 206−215.
(37) Hess, B.; Kutzner, C.; van der Spoel, D.; Lindahl, E. GROMACS 4: Algorithms for Highly Efficient, Load-Balanced, and Scalable Molecular Simulation. *J. Chem. Theory Comput.* **2008**, *4*, 435−447.
(38) Jorgensen, W. L.; McDonald, N. A. Development of an All-Atom Force Field for Heterocycles. Properties of Liquid Pyridine and Diazenes. *J. Mol. Struct. (Theochem)* **1998**, *424*, 145−155.
(39) Sabbah, R.; Chastel, R.; Laffitte, M. Étude Thermochimique des Méthylnaphtalènes. *Thermochim. Acta* **1974**, *10*, 353−358.
(40) Latif, H. A.; Khalid, A. A.; Jasim, M. A. Chemical Structure of Asphaltenes in Heavy Crude Oils Investigated by NMR. *Fuel* **1990**, *69*, 519−521.
(41) Ovalles, C.; Rogel, E.; Moir, M.; Thomas, L.; Pradhan, A. Characterization of Heavy Crude Oils, Their Fractions, and Hydrovisbroken Products by the Asphaltene Solubility Fraction Method. *Energy Fuels* **2012**, *26*, 549−556.
(42) Sun, Y.; Yang, C.; Zhao, H.; Shan, H.; Shen, B. Influence of Asphaltene on the Residue Hydrotreating Reaction. *Energy Fuels* **2010**, *24*, 5008−5011.
(43) Douda, J.; Alvarez, R.; Navarrete Bolaños, J. Characterization of Maya Asphaltene and Maltene by Means of Pyrolysis Application. *Energy Fuels* **2008**, *22*, 2619−2628.
(44) Calemma, V.; Iwanski, P.; Nali, M.; Scotti, R.; Montanari, L. Structural Characterization of Asphaltenes of Different Origins. *Energy Fuels* **1995**, *9*, 225−230.
(45) Trejo, F.; Ancheyta, J.; Morgan, T. J.; Herod, A. A.; Kandiyoti, R. Characterization of Asphaltenes from Hydrotreated Products by SEC, LDMS, MALDI, NMR, and XRD. *Energy Fuels* **2007**, *21*, 2121−2128.
(46) Ibrahim, H. H.; Idem, R. O. Correlations of Characteristics of Saskatchewan Crude Oils/Asphaltenes with Their Asphaltenes Precipitation Behavior and Inhibition Mechanisms: Differences between CO2- and n-Heptane-Induced Asphaltene Precipitation. *Energy Fuels* **2004**, *18*, 1354−1369.
(47) Kästner, J. Umbrella Sampling. *WIREs Comput. Mol. Sci.* **2011**, *1*, 932−942.

(48) Kumar, S.; Bouzida, D.; Swendsen, R. H.; Kollman, P. A.; Rosenberg, J. M. THE Weighted Histogram Analysis Method for Free-Energy Calculations on Biomolecules. I. The Method. *J. Comput. Chem.* **1992**, *13*, 1011−1021.
(49) Hub, J. S.; de Groot, B. L.; van der Spoel, D. g_wham−A Free Weighted Histogram Analysis Implementation Including Robust Error and Autocorrelation Estimates. *J. Chem. Theory Comput.* **2010**, *6*, 3713−3720.
(50) Roux, B. The Calculation of the Potential of Mean Force Using Computer Simulations. *Comput. Phys. Commun.* **1995**, *91*, 275−282.
(51) Apol, E.; Apostolov, R.; Berendsen, H. J. C.; van Buuren, A. R.; Bjelkmar, P.; Drunen, R.; Feenstra, K. A.; Groenhof, G.; Kasson, P.; Larsson, P.; Meulenhoff, P. J.; Murtola, T.; Páll, S.; Pronk, S.; Schulz, R.; Shirts, M.; Sijbers, A. L. T. M.; Tieleman, D. P.; Hess, B.; van der Spoel, D.; Lindahl, E. *Gromacs User Manual*, version 4.5.4, 2010; www.gromacs.org.
(52) Neumann, R. M. Entropic Approach to Brownian Movement. *Am. J. Phys.* **1980**, *48*, 354−357.
(53) Rogel, E. Molecular Thermodynamic Approach to the Formation of Mixed Asphaltene-Resin Aggregates. *Energy Fuels* **2008**, *22*, 3922−3929.
(54) Li, D. D.; Greenfield, M. L. High Internal Energies of Proposed Asphaltene Structures. *Energy Fuels* **2011**, *25*, 3698−3705.
(55) *Asphaltenes and Asphalts*; Yen, T. F., Chilingarian, G. V., Eds.; Elsevier Scientific Publishing Co.: Amsterdam, The Netherlands, 1994; Vol. *1*, Chap. 2.
(56) Wattana, P.; Fogler, S.; Yen, A.; Garcia, M. D. C.; Carbognani, L. Characterization of Polarity-Based Asphaltene Subfractions. *Energy Fuels* **2005**, *19*, 101−110.
(57) Klein, G. C.; Kim, S.; Rodgers, R. P.; Marshall, A. G. Mass Spectral Analysis of Asphaltenes. II. Detailed Compositional Comparison of Asphaltenes Deposit to Its Crude Oil Counterpart for Two Geographically Different Crude Oils by ESI FT-ICR MS. *Energy Fuels* **2006**, *20*, 1973−1979.
(58) Sedghi, M.; Goual, L. Role of Resins on Asphaltene Stability. *Energy Fuels* **2010**, *24*, 2275−2280.
(59) *Equations of State for Fluids and Fluid Mixures*; Sengers, J. V., Kayser, R. F., Peters, C. J., Whiter, H. J. Jr., Eds.; Elsevier Scientific Publishing Co.: Amsterdam, The Netherlands, 2000; Chapter 15.